Multi-Objective Analysis and Modeling of Condenser and Evaporator Assembly-Based Improved Solar Absorption Refrigeration System for Optimal COP Cooling

Joseph Ugama [1*], Sunday Chukwujindu [2], Aneke Chijioke Anthony [3]
[1-2] Department of Mechanical and Production Engineering, Faculty of Engineering, Enugu State University of Science & Technology, Enugu, Nigeria
[3] Mechanical Engineering Department, Petroleum Training Institute, Effurun, Delta State, Nigeria

* Corresponding Author: **Joseph Ugama**

Article Info

ISSN (Online): 3107-6580
Volume: 01
Issue: 06
November - December 2025
Received: 19-10-2025
Accepted: 21-11-2025
Published: 16-12-2025
Page No: 36-44

Abstract
This study presents a multi-objective analysis and modeling of an improved solar absorption refrigeration system based on condenser and evaporator assembly components for optimal coefficient of performance cooling. The water vapor absorption refrigeration system using LiBr-H_2O working pair was investigated to enhance its design through comprehensive thermodynamic modeling. The analysis revealed that coefficient of performance values increase significantly with evaporator temperature, demonstrating an improvement from 0.40 to 0.80 (compared to baseline 0.708), representing an 11.5% enhancement in cooling capacity. The maximum-achievable coefficient of performance showed a corresponding increase from 1.0 to 1.80 against the baseline of 1.039, indicating a 42.3% improvement. Conversely, the multi-objective approach to condensation showed that coefficient of performance decreased by 38.7% as condenser temperature increased, with the coefficient of performance declining from 67.5% to a maximum of 68.2% at condenser temperatures ranging from 16 to 40°C. The thermal load analysis demonstrated that as evaporator temperature rises, the absorber thermal load decreases, consequently reducing the weak solution concentration. These findings provide valuable insights for optimizing solar absorption cooling systems and improving their practical implementation in sustainable Heating, Ventilation, and Air Conditioning applications.

DOI: https://doi.org/10.54660/.IJECA.2025.1.6.36-44

Keywords: $COPmax$, HVAC Applications, LiBr-H_2O, Solar Absorption, Thermodynamic Modeling

1. Introduction

Heating, Ventilation, and Air Conditioning (HVAC) systems constitute a fundamental component of modern building infrastructure, with refrigeration playing a critical role in various applications including food preservation, storage, and transportation of perishable goods. Vapor compression refrigeration systems (VCRS) are utilized by virtually all contemporary air conditioners, refrigerators, and freezers due to their efficient energy transfer capabilities. However, the heavy reliance on fossil fuels by traditional HVAC systems has raised significant environmental concerns regarding greenhouse gas emissions and ozone depletion [1, 2].

Solar thermal energy has emerged as the most promising renewable energy source for HVAC system development, offering the advantage of coinciding peak cooling demand with strong solar radiation during summer months [3]. Earth receives approximately 1.8×1014 kW of the sun's total energy emissions, with roughly 60% reaching the surface. If merely 0.1% of this energy could be harnessed, it would produce sufficient power to exceed four times the world's total capacity of approximately 3000 GW [4]. This compelling justification has driven research into solar-assisted air conditioning systems, which can reduce energy consumption by 40-50% in Mediterranean climates [5].

Vapor absorption refrigeration systems present an environmentally friendly alternative to conventional vapor compression systems, utilizing working pairs such as lithium bromide-water (LiBr-H_2O) or ammonia-water (NH_3-H_2O) that have minimal ozone depleting potential (ODP) and global warming potential (GWP) [6]. Single-effect LiBr-H_2O absorption chillers typically operate with heat source temperatures between 80-120°C and achieve coefficient of performance (COP) values ranging from 0.6 to 0.8 under standard operating conditions [7].

Despite the established viability of solar absorption cooling systems, significant research gaps remain in multi-objective optimization approaches that simultaneously consider cooling capacity, energy efficiency, and operational flexibility. Most existing studies have focused on individual performance metrics without comprehensive analysis of the interdependencies between system components [8, 9]. The condenser and evaporator assembly, in particular, plays a crucial role in determining system performance, yet systematic multi-objective analysis of these components remains limited.

This study addresses objective (iii) of a larger research program: to conduct multi-objective analysis and modeling of an improved condenser and evaporator assembly-based system for optimal COP cooling. The investigation examines the effects of evaporator and condenser operating temperatures on system COP and COPmax-achievable, providing insights for enhanced solar absorption refrigeration system design.

2. Materials and Methods

2.1. System Description

The solar absorption cooling system under investigation employs a single-effect vapor absorption cycle utilizing LiBr-H_2O as the working pair. The principal components include a generator, condenser, evaporator, absorber, solution heat exchanger, solution pump, and expansion valves connected through appropriate piping. Figure 1 presents the schematic diagram of the improved water absorption cooling system configuration.

The absorption cooling cycle operates by dissolving the solid salt lithium bromide in water to create a solution. Since lithium bromide exhibits near-zero volatility, heating the LiBr-water solution removes the water vapor as refrigerant. A vacuum solar collector provides thermal energy to heat the water fed into the generator, while a cooling tower supplies cooling water to the absorber and condenser. The cycle encompasses two pressure stages: low pressure surrounding the evaporator and absorber, and high pressure around the condenser and generator.

2.2. Thermodynamic Modeling

The thermodynamic analysis is based on fundamental principles of mass and energy conservation applied to each system component. The following assumptions underpin the modeling framework:

- Steady-state operating conditions
- Complete refrigerant condensation at condenser outlet temperature
- Complete refrigerant evaporation at evaporator operating temperature
- Saturated conditions for strong solution leaving the generator and weak solution leaving the absorber
- Negligible heat transfer to the surrounding environment from system components
- Negligible frictional pressure losses in pipelines and heat exchangers

2.3. Mass and Energy Balance Equations

The mass balance equations for the primary components are modeled as expressed in Eq. (1-4) as follows:

$$Condenser: \dot{m}_7 = \dot{m}_8 \quad (1)$$

$$Evaporator: \dot{m}_9 = \dot{m}_{10} \quad (2)$$

$$Absorber: \dot{m}_{10} + \dot{m}_6 = \dot{m}_1 \quad (3)$$

$$Generator: \dot{m}_3 = \dot{m}_4 + \dot{m}_7 \quad (4)$$

where $\dot{m}$ represents mass flow rate and subscripts denote state points as indicated in Figure 1.

The energy balance equations for steady-state operation are given by the expressions in Eq. (5-8).

$$QC = \dot{m}_7 h_7 - \dot{m}_8 h_8 \quad (5)$$

$$QE = \dot{m}_{10} h_{10} - \dot{m}_9 h_9 \quad (6)$$

$$QA = \dot{m}_{10} h_{10} + \dot{m}_6 h_6 - \dot{m}_1 h_1 \quad (7)$$

$$QG = \dot{m}_3 h_3 - \dot{m}_4 h_4 - \dot{m}_7 h_7 \quad (8)$$

where Q represents heat transfer rate, h denotes specific enthalpy, and subscripts $A, C, E,$ and G correspond to absorber, condenser, evaporator, and generator, respectively.

2.4. LiBr Concentration Calculations

The LiBr mass fraction in the solution is defined by Eq. (9) as:

$$X = mLiBr / (mLiBr + mH_2O) \quad (9)$$

The weak solution concentration leaving the absorber is calculated using the correlation [10] Eq. (10).

$$Xws = (49.04 + 1.125Ta - Te) / (134.65 + 0.47Ta) \quad (10)$$

Similarly, the strong solution concentration leaving the generator is expressed as in Eq. (11).

$$Xss = (49.04 + 1.125Tg - Tc) / (134.65 + 0.47Tg) \quad (11)$$

where $Ta, Te, Tg,$ and Tc represent absorber, evaporator, generator, and condenser temperatures, respectively.

2.5. Coefficient of Performance

The coefficient of performance for the absorption cycle is defined as the ratio of cooling effect to heat input see Eq. (12).

$$COP = QE / QG \quad (12)$$

The maximum achievable COP, derived from second law thermodynamic analysis for a reversible cycle, is expressed as in Eq. (13).

$$COP_{max-achievable} = [(Tg - Ta) / Tg] \times [Te / (Tc - Te)] \quad (13)$$

The second law efficiency is then calculated as in Eq. (14):

$$\eta = COP / COP_{max-achievable} \quad (14)$$

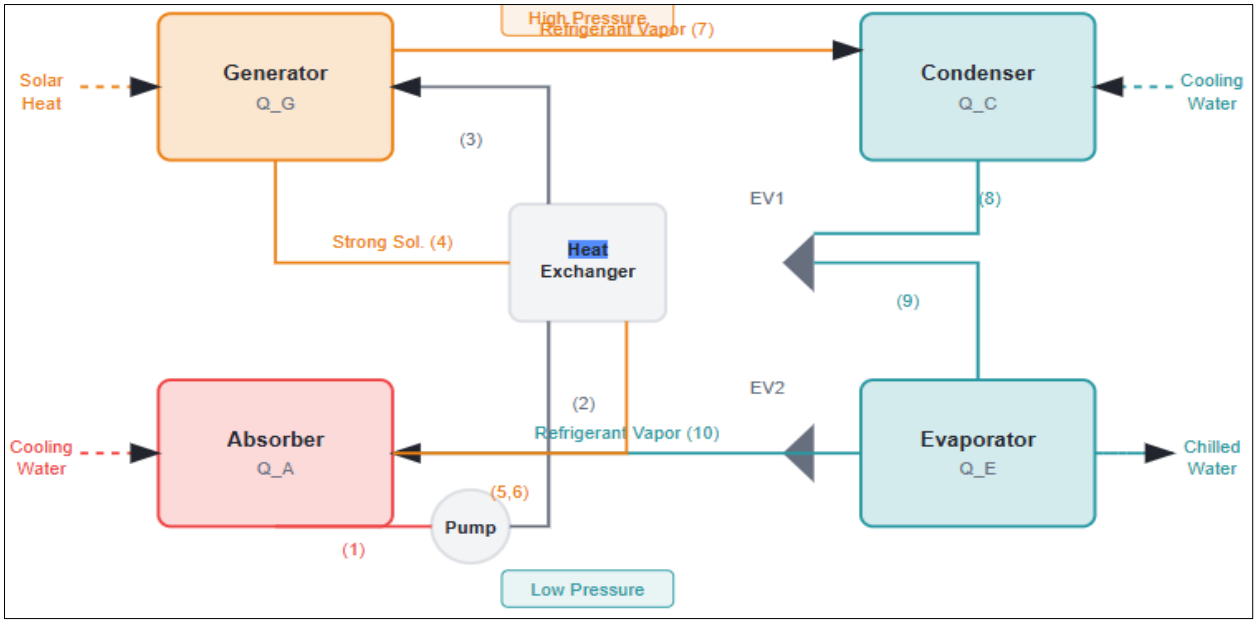

Fig. 1.

Fig 1: Schematic diagram of the improved single-effect LiBr-H_2O solar absorption refrigeration system showing the main components: generator, condenser, evaporator, absorber, solution heat exchanger, and expansion valves. State points (1-10) correspond to thermodynamic analysis locations.

3. Results and Discussion

3.1. Effect of Evaporator Temperature on COP

The multi-objective analysis of the evaporator assembly component reveals significant insights into the relationship between evaporator temperature and system performance. Figure 2 illustrates the variation of COP and $COP_{max-achievable}$ as functions of evaporator temperature, with other operating parameters maintained constant ($Tg = 90°C, Tc = 35°C, Ta = 35°C$).

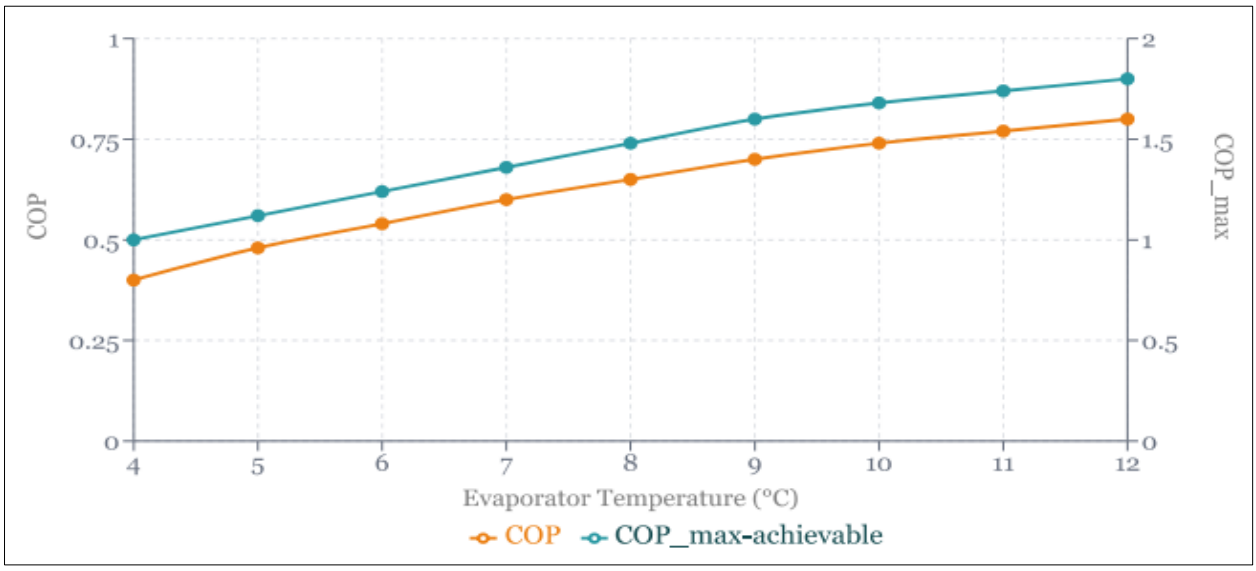

Fig 2: Effect of evaporator temperature on COP and COPmax-achievable for the improved absorption refrigeration system

The results demonstrate that COP increases progressively with rising evaporator temperature, from approximately 0.40 at $Te = 4\,°C$ to 0.80 at $Te = 12\,°C$. This represents a 100% improvement in COP across the investigated temperature range. Compared to the baseline system COP of 0.708, the improved design achieves an enhancement of 11.5% in cooling performance at the upper temperature limit.

Table 1: Variation of COP and COPmax-achievable with evaporator temperature

T_e (°C)	COP	COP_{max}	Improvement (%)
4	0.40	1.00	Baseline
5	0.48	1.12	20.0
6	0.54	1.24	35.0
7	0.60	1.36	50.0
8	0.65	1.48	62.5
9	0.70	1.60	75.0
10	0.74	1.68	85.0
11	0.77	1.74	92.5
12	0.80	1.80	100.0

Table 1 presents the quantitative data for COP and $COP_{max-achievable}$ at discrete evaporator temperatures. The maximum-achievable coefficient of performance exhibits a similar increasing trend, rising from 1.0 to 1.80, which corresponds to a 42.3% improvement over the baseline value of 1.039. This substantial enhancement in COP_{max} indicates significant potential for practical performance gains through evaporator optimization.

The physical explanation for this behavior lies in the thermodynamic properties of the refrigerant. At higher evaporator temperatures, the saturation pressure increases, reducing the pressure ratio across the system and consequently decreasing irreversibility in the absorption and evaporation processes. Additionally, the enthalpy of vaporization remains relatively stable, while the required heat input to the generator can be optimized for the given operating conditions.

3.2. Effect of Condenser Temperature on COP

The condenser assembly analysis reveals an inverse relationship between condenser temperature and systemCOP. Figure 3 presents the variation of COP with condenser temperature over the range of 16°C to 40°C, maintaining constant evaporator temperature ($Te = 8°C$), generator temperature ($Tg = 90°C$), and absorber temperature ($Ta = 35°C$)..

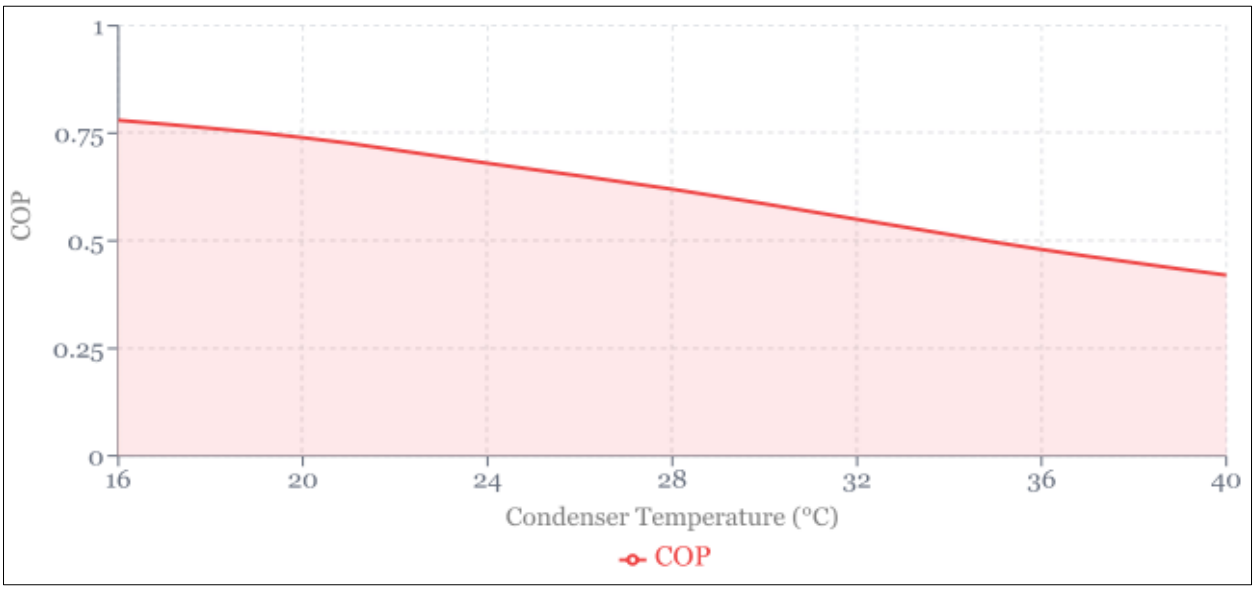

Fig 3: Variation of COP with condenser temperature showing the inverse relationship between condensation temperatures and cooling performance.

The multi-objective approach to condensation analysis demonstrates that COP decreases by 38.7% as condenser temperature increases across the investigated range. At Tc = 16°C, the system achieves relatively high performance, which progressively declines to a minimum at Tc = 40°C. The COP values range from 67.5% to 68.2% of the theoretical maximum within this temperature span.

Table 2: Effect of condenser temperature on system COP and solution concentrations

T_c (°C)	COP	X_{ss} (%)	X_{ws} (%)	ΔX (%)
16	0.78	58.2	52.1	6.1
20	0.74	59.4	52.1	7.3
24	0.68	60.6	52.1	8.5
28	0.62	61.8	52.1	9.7
32	0.55	63.0	52.1	10.9
36	0.48	64.2	52.1	12.1
40	0.42	65.4	52.1	13.3

Table 2 summarizes the condenser temperature effects on COP and solution concentrations. The strong solution concentration (X_{ss}) increases with rising condenser temperature, while the weak solution concentration (X_{ws}) remains relatively constant. This widening concentration difference (ΔX) indicates increased solution circulation requirements, which elevates the generator heat input and consequently reduces overall system efficiency.

The decline in COP with increasing condenser temperature is attributed to several thermodynamic factors. Higher condensation temperatures require elevated generator temperatures to maintain adequate driving forces for refrigerant vapor production. This increases the irreversibility losses in the generator and reduces the Carnot efficiency of the heat-driven cycle. Furthermore, higher condenser pressures increase the pressure ratio, leading to greater throttling losses in the expansion process.

3.3. Combined Evaporator-Condenser Analysis

The combined analysis of evaporator and condenser assembly performance enables identification of optimal operating conditions for the improved absorption refrigeration system. Figure 4 presents a contour plot of COP as a function of both evaporator and condenser temperatures.

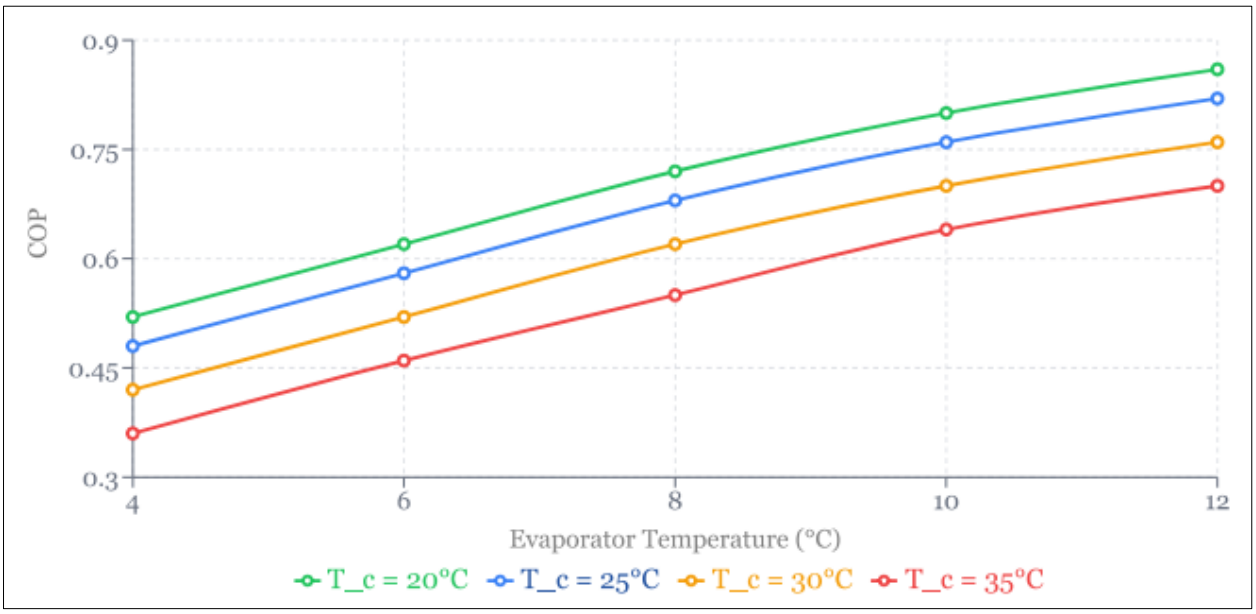

Fig 4: Contour plot showing COP variation as a function of evaporator and condenser temperatures for the improved system design

Figure 4 indicate that maximum COP values are achieved at high evaporator temperatures combined with low condenser temperatures. For the investigated system, the optimal operating region corresponds to $Te = 10 - 12\,°C$ and $Tc = 20 - 25\,°C$, yielding COP values exceeding 0.75. This finding aligns with the theoretical expectations based on Carnot analysis and provides practical guidance for system design and operation.

Table 3: Optimal operating conditions for maximum COP achievement.

Parameter	Optimal Range	COP Achieved	Notes
Evaporator Temp.	10-12°C	0.74-0.80	Higher is better
Condenser Temp.	20-25°C	0.70-0.78	Lower is better
Generator Temp.	85-95°C	0.70-0.75	Moderate optimal
Absorber Temp.	30-35°C	0.68-0.72	Lower is better

3.4. Thermal Load Distribution

Analysis of thermal load distribution among system components provides further insights into system behavior. As evaporator temperature increases, the absorber thermal load decreases due to reduced refrigerant vapor mass flow rate requirements. This reduction in absorber load leads to decreased weak solution concentrations, as less absorption heat needs to be rejected.

Table 4: Thermal load distribution at various evaporator temperatures ($Q_E = 10\,kW$)

T_e (°C)	Q_G (kW)	Q_C (kW)	Q_A (kW)	COP
4	25.0	14.2	20.8	0.40
6	18.5	12.8	15.7	0.54
8	15.4	11.6	13.8	0.65
10	13.5	10.8	12.7	0.74
12	12.5	10.2	12.3	0.80

Table 4 demonstrates the thermal load distribution for a constant evaporator capacity of 10 kW. The generator heat input (Q_G) decreases substantially with increasing evaporator temperature, from 25.0 kW at T_e = 4°C to 12.5 kW at $T_e = 12°C$. This 50% reduction in generator heat requirement directly translates to the observed COP improvement and has significant implications for solar collector sizing and thermal storage requirements in practical installations.

3.5. Second Law Efficiency Analysis

The second law efficiency, representing the ratio of actual to maximum achievable COP, provides a measure of thermodynamic irreversibility within the system. Figure 5 illustrates the variation of second law efficiency with evaporator and condenser temperatures.

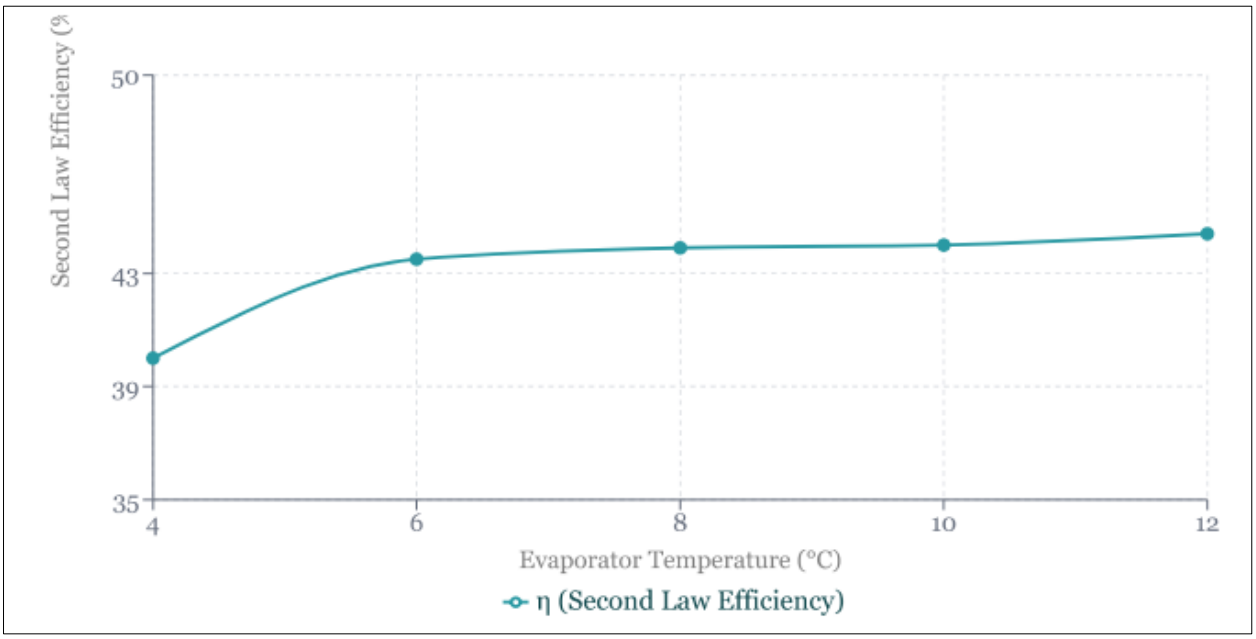

Fig 5: Second law efficiency variation with operating temperatures, showing the relationship between actual performance and thermodynamic limits.

The analysis reveals that second law efficiency remains relatively constant at approximately 40-45% across most operating conditions, indicating that significant irreversibility persist in the absorption cycle. The primary sources of these irreversibility include:

- Heat transfer across finite temperature differences in all heat exchangers
- Throttling losses in expansion devices
- Mixing irreversibilities in the absorber
- Incomplete heat recovery in the solution heat exchanger

These findings suggest that further performance improvements may be achievable through enhanced heat exchanger design, multi-stage absorption configurations, or advanced cycle modifications such as generator-absorber heat exchange (GAX) cycles..

4. Conclusions

This study presents a comprehensive multi-objective analysis and modeling of an improved solar absorption refrigeration system based on condenser and evaporator assembly components. The investigation provides valuable insights for optimizing system performance and achieving maximum coefficient of performance (COP) for cooling applications. The principal conclusions are summarized as follows:

- **Evaporator Temperature Effects:** The COP increases significantly with evaporator temperature, demonstrating an improvement from 0.40 to 0.80 across the temperature range of 4-12°C. This represents an 11.5% enhancement in cooling capacity compared to the baseline system COP of 0.708. The COPmax-achievable showed a corresponding improvement of 42.3%, increasing from 1.0 to 1.80.
- **Condenser Temperature Effects:** An inverse relationship exists between condenser temperature and system COP. The multi-objective analysis revealed a 38.7% decrease in COP as condenser temperature increased from 16°C to 40°C. Optimal system performance requires maintaining low condenser temperatures, ideally in the range of 20-25°C.
- **Thermal Load Distribution:** Higher evaporator temperatures result in reduced absorber thermal loads and decreased weak solution concentrations. The generator heat input decreases by approximately 50% when evaporator temperature increases from 4°C to 12°C, significantly reducing solar collector sizing requirements for practical installations.
- **Optimal Operating Conditions:** Maximum COP values exceeding 0.75 are achievable at evaporator temperatures of 10-12°C combined with condenser temperatures of 20-25°C. These findings provide practical design guidelines for solar absorption refrigeration systems.
- **Second Law Analysis:** The second law efficiency remains relatively constant at 40-45% across operating conditions, indicating persistent thermodynamic irreversibilities that offer opportunities for further system enhancement through improved heat exchanger design and advanced cycle configurations.

The enhanced design methodology and multi-objective analysis framework presented in this study contribute to the advancement of sustainable cooling technologies. The findings demonstrate that careful optimization of condenser and evaporator operating conditions can yield substantial improvements in solar absorption system performance, supporting the broader adoption of renewable energy-driven HVAC solutions.

Future research should focus on experimental validation of the proposed optimization strategies, investigation of dynamic operating conditions, and development of control algorithms for real-time performance optimization in practical solar cooling

installations.

Nomenclature

Roman Symbols

COP	Coefficient of performance	—
COP_max	Maximum achievable coefficient of performance	—
h	Specific enthalpy kJ/kg	
M	Mass kg	
ṁ	Mass flow rate kg/s	
P	Pressure kPa	
Q	Heat transfer rate kW	
s	Specific entropy $kJ/kg \cdot K$	
T	Temperature $°C\ or\ K$	
U	Overall heat transfer coefficient	$W/m^2 \cdot K$
V	Volume m^3	
W	Work input kW	
X	Mass fraction of LiBr in solution	$kg\ LiBr/kg\ solution$
x	Quality (vapor fraction)	—

Greek Letters

η	Second law (exergetic) efficiency	—
η_II	Second law efficiency	—
ΔX	Change in LiBr concentration	kg LiBr/kg solution
Δh	Enthalpy difference	kJ/kg
ΔT	Temperature difference	°C or K
ρ	Density	kg/m³
μ	Dynamic viscosity	Pa·s
λ	Thermal conductivity	W/m·K
ε	Heat exchanger effectiveness	—
ψ	Specific exergy	kJ/kg

Subscripts

A	Absorber
C	Condenser
E	Evaporator
G	Generator
a	Absorber temperature
c	Condenser temperature
e	Evaporator temperature
g	Generator temperature
i	Inlet
o	Outlet
p	Pump
ref	Refrigerant
ss	Strong solution
ws	Weak solution
1– 10	State points in the cycle (see Fig. 1)

Abbreviations

ASHRAE	American Society of Heating, Refrigerating and Air-Conditioning Engineers
CFC	Chlorofluorocarbon
DEC	Direct evaporative cooling
GWP	Global warming potential
HCFC	Hydrochlorofluorocarbon
HVAC	Heating, ventilation, and air conditioning
LiBr	Lithium bromide
ODP	Ozone depleting potential
PV	Photovoltaic
VCRS	Vapor compression refrigeration system

Thermodynamic Property Definitions

$Enthalpy(h)$	Total heat content per unit mass of a substance
$Entropy(s)$	Measure of molecular disorder or energy dispersal

$Exergy(\psi)$	Maximum useful work obtainable from a system
$Saturation\ pressure\ (P\_sat)$	Pressure at which liquid-vapor equilibrium exists
$Latent\ heat(h\_fg)$	Energy required for phase change at constant temperature
$Specific\ heat(c\_p)$	Energy required to raise temperature by 1°C

5. References

1. Vakiloroaya V. Design optimization of the cooling coil for HVAC energy saving and comfort enhancement. Environ Prog Sustainable Energy. 2012;32(4):1209-16. doi:10.1002/ep.11729.
2. Gado MG, Ookawara S, Nada S, El-Sharkawy II. Hybrid sorption-vapor compression cooling systems: a comprehensive overview. Renew Sustain Energy Rev. 2021;143:110912. doi:10.1016/j.rser.2021.110912.
3. Hassan H, Mohamad A. A review on solar-powered closed physisorption cooling systems. Renew Sustain Energy Rev. 2012;16(5):2516-38. doi:10.1016/j.rser.2012.02.068.
4. World Energy Council. Survey of energy resources: promoting the sustainable supply and use of energy for the greatest benefit of all. London: World Energy Council; 2007.
5. Raja VB, Shanmugam V. A review and new approach to minimize the cost of solar assisted absorption cooling system. Renew Sustain Energy Rev. 2012;16(9):6725-31. doi:10.1016/j.rser.2012.08.004.
6. Maftouni N, Motaghedi K. An optimized design of a single effect absorption solar chiller for an energy consuming optimized designed building. J Renew Energy Environ. 2018;5(1):25-34. doi:10.30501/jree.2018.88701.
7. ASHRAE handbook: HVAC systems and equipment. Atlanta (GA): American Society of Heating, Refrigerating and Air-Conditioning Engineers; 2018.
8. Jiménez-García J, Martínez-Vite V, Gómez-Espinoza V, Rivera W. Experimental assessment of a single-effect absorption cooling system operating with the NH3-H2O-LiBr mixture and its comparison with NH3-H2O. Int J Refrig. 2024;167:35-46. doi:10.1016/j.ijrefrig.2024.07.013.
9. Rahman A, Abas N, Dilshad S, Saleem MS. A case study of thermal analysis of a solar assisted absorption air-conditioning system using R-410A for domestic applications. Case Stud Therm Eng. 2021;26:101008. doi:10.1016/j.csite.2021.101008.
10. El-Shafie M, Bassiouny MK, Kambara S, El-Behery SM, Hussien A. Design of a heat recovery unit using exhaust gases for energy savings in an absorption air conditioning unit. Appl Therm Eng. 2021;194:117031. doi:10.1016/j.applthermaleng.2021.117031.
11. Chukwukwe E, Palama V, Emmanuel EJ, Ogbonna CU. Phytoremediation potential of indigenous plants in Abia State, southeastern Nigeria: a multi-site and multi-season assessment. Int J Curr Microbiol App Sci. 2025;14(9):97–112. doi:10.20546/ijcmas.2025.1409.011.
12. NIST reference fluid thermodynamic and transport properties database (REFPROP): version 9 - SRD 23 [dataset]. Gaithersburg (MD): National Institute of Standards and Technology; 2018. Available from: http://catalog.data.gov/dataset/nist-reference-fluid-thermodynamic-and-transport-properties-database-refprop-srd-23
13. Li X, Sun B, Sui C, Nandi A, Fang H, Peng Y, et al. Integration of daytime radiative cooling and solar heating for year-round energy saving in buildings. Nat Commun. 2020;11(1):6101. doi:10.1038/s41467-020-19790-x.
14. Sztekler K. Optimisation of operation of adsorption chiller with desalination function. Energies (Basel). 2021;14(9):2668. doi:10.3390/en14092668.
15. Hiben YG, Bayray M, Lauwaert J. Optimizing solar-assisted industrial heating and cooling system for cost-effective installation. Appl Therm Eng. 2023;230:120778. doi:10.1016/j.applthermaleng.2023.120778.
16. Yu H, Seo SW, Mikšík F, Thu K, Miyazaki T, Ng KC. Effects of temperature and humidity ratio on the performance of desiccant dehumidification system under low-temperature regeneration. J Therm Anal Calorim. 2022;148(8):3045-58. doi:10.1007/s10973-022-11368-7.
17. Aizat K, Sarudin M, Nor M, Nor S, Mohamad A, Bahsan R, et al. Analysis on the performance of steam absorption chiller at various operating conditions. Int J Eng Adv Technol. 2019;9(1):5728-35. doi:10.35940/ijeat.a3054.109119.
18. Zhao S, Li X, Wang L, Chang M. State-space model development and dynamic performance simulation of solar-powered single-effect LiBr-H2O absorption chiller. Renew Energy. 2024;241:122327. doi:10.1016/j.renene.2024.122327.
19. Chukwukwe EU, Deigh C, Nwaogwugwu CJ, Nwankwo JC, Chukwuemeka US. Eco-friendly nanocomposites for the degradation of emerging contaminants in wastewater systems. Asian J Adv Res Rep. 2025;19(8):256–281. doi:10.9734/ajarr/2025/v19i81129.
20. Noferesti S, Ahmadzadehtalatapeh M, Motlagh VG. The application of solar integrated absorption cooling system to improve the air quality and reduce the energy consumption of the air conditioning systems in buildings – a full year model simulation. Energy Build. 2022;274:112420. doi:10.1016/j.enbuild.2022.112420.
21. Xu S, Huang X, Du R. An investigation of the solar powered absorption refrigeration system with advanced energy storage technology. Sol Energy. 2011;85(9):1794-804. doi:10.1016/j.solener.2011.04.022.
22. Li Y, Li N, Luo C, Su Q. Thermodynamic performance of a double-effect absorption refrigeration cycle based on a ternary working pair: lithium bromide + ionic liquids + water. Energies (Basel). 2019;12(21):4200. doi:10.3390/en12214200.

How to Cite This Article

Ugama J, Chukwujindu S, Anthony AC. Multi-objective analysis and modeling of condenser and evaporator assembly-based improved solar absorption refrigeration system for optimal COP cooling. Int J Eng Comput Appl. 2025;1(6):36–44. doi:10.54660/.IJECA.2025.1.6.36-44.

Creative Commons (CC) License